Separation Science and Technology
Publication details, including instructions for authors and subscription information:
http://www.informaworld.com/smpp/title~content=t713708471

Short-Fiber Chromatography Columns: Potential for Process-Scale Bioseparations

Chad A. Farschman[a]; John B. Manos[a]; Neville G. Pinto[a]
[a] Department of Chemical Engineering, University of Cincinnati, Cincinnati, OH

To cite this Article Farschman, Chad A. , Manos, John B. and Pinto, Neville G.(1995) 'Short-Fiber Chromatography Columns: Potential for Process-Scale Bioseparations', Separation Science and Technology, 30: 7, 1325 — 1350
To link to this Article: DOI: 10.1080/01496399508010349
URL: http://dx.doi.org/10.1080/01496399508010349

SEPARATION SCIENCE AND TECHNOLOGY, 30(7-9), pp. 1325-1350, 1995

SHORT-FIBER CHROMATOGRAPHY COLUMNS: POTENTIAL FOR PROCESS-SCALE BIOSEPARATIONS

Chad A. Farschman, John B. Manos and Neville G. Pinto*
Department of Chemical Engineering
University of Cincinnati
Mail Location 0171
Cincinnati, OH 45221-0171

ABSTRACT

Chromatographic supports with short-fiber geometry have been evaluated for process-scale applications. Using a prototype silica-based ion-exchange fiber and bovine serum albumin as the model biomolecule, a comparison of the throughput characteristics of fiber columns with those of conventional columns (spherical packing) has been made. The comparison accounts for the influences of pressure drop, adsorption thermodynamics, and mass transfer. It has been shown that retention characteristics, mass dispersion, and intraparticle mass-transfer resistance are critical in determining which column has a higher throughput. In general, if the capacity factor of the desired product is high, it is predicted that the fiber column will give higher throughputs, except for separations that involve closely eluting impurities. Based on these results, guidelines detailing desired properties of short-fiber chromatographic supports are provided.

INTRODUCTION

The importance of developing efficient, simple, and economical separation techniques for downstream processing of bioproducts has been recognized for some time (1). Effluents from cell culture bioreactors are generally dilute solutions of the

desired bioproduct(s) in a complex mixture of very similar components. Consequently, involved multistep separation protocols are necessary to achieve product purification.

Liquid chromatography is used extensively in downstream separation protocols, particularly for product purification and final polishing. The strength of this technique is its inherent ability to pack a large number of equilibrium separation stages in a small volume, making it possible to efficiently separate virtually identical compounds. However, because current process-scale chromatographic systems are essentially direct scaled-up versions of corresponding bench-scale analytical units, their performance is far from optimal. Operational experience has shown that direct scale-up leads to a decrease in separation efficiency for a number of reasons (2). For example, analytical columns generally use spherical packing with diameters in the range of 5-30 μm and a tight size distribution. The primary advantage of using small particles is a decrease in the mass-transfer resistance in the stationary phase, and a consequent sharpening of concentration peaks. A tight size distribution minimizes nonuniform regions in the column with respect to void fraction and, thus, decreases band broadening due to dispersion caused by mixing. However, the high cost of analytical packing does not make it practical for process-scale applications. Packing used in this case has diameters ranging from 40-300 μm and a much wider size distribution, resulting in poorer column performance.

Small particles in process-scale units also impose an upper limit on the length of the column, due to the attendant pressure drop. In order to circumvent this limitation, the scale-up of analytical units is achieved by increasing the column diameter without significantly increasing column length (3). While this maintains the crushing forces on the solid at acceptable levels, it leads to other problems such as uneven flow distribution in the column and nonuniform sample distribution and product collection (4).

In order to improve the efficiency of process-scale liquid chromatography, a number of promising new configurations have been proposed or are under investigation (5-8). Of particular interest are randomly packed short-fiber (RPSF) columns. These columns are identical to conventional chromatographic columns, except that they are packed with short, fibrous supports instead of spherical materials. Initial investigations with RPSF columns packed with activated silica fibers (9,10) have shown that these columns exhibit a significantly lower pressure drop than conventional columns, and the separation of biomolecules can be achieved at elevated flow rates. Also, recent work with porous polymeric fibers (11) has demonstrated that the capacity of RPSF columns can be made to rival that of conventional columns.

The major implication of the above characteristics of RPSF columns is that mass transport within the stationary phase can be made much more efficient, since fibers with diameters in the submicron range can be used without generating excessive pressure drops in the column. This is a significant advantage over spherical supports, which are limited by viscous heating effects to sizes larger than 2 μm (12). However, this does not guarantee that RPSF columns will be superior to conventional columns with respect to product throughput and recovery. As has been pointed out earlier, because fibrous supports have a lower symmetry than spherical supports (10), flow dispersion effects can be significant. This will tend to counter the advantage gained from more efficient mass transfer. Thus, the effects of operating and thermodynamic conditions on flow dispersion and mass transfer must be considered in order to establish under what conditions, if any, RPSF columns will prove to be advantageous.

In this paper, the results of a theoretical comparison of the performance characteristics of an RPSF column and a conventional column packed with spherical supports have been presented. Using a prototype silica ion-exchange fiber, dispersion characteristics in RPSF columns were measured. These data, in conjunction with equilibrium adsorption data for a commercial ion-exchange support,

have been used in a simulation model to compare separation performance as a function of difficulty of separation, mobile phase velocity, and column length.

MODEL

In order to compare the throughputs attainable in conventional and RPSF columns, the model of Knox and Pyper (13) was used. Though this model does not account for interactions between migrating zones in the overloaded mode and approximates the shape of the bands as right triangular, Snyder and co-workers (14) have found that it gives qualitatively correct predictions of column behavior as long as the mass of any sample component does not exceed 5% of the column capacity. In the Knox and Pyper model, the throughput of a column is given by:

$$T = \left[\frac{L}{N^*} - H(u)\right] \frac{4(1+k^o)}{\beta\, t_m} \quad . \tag{1}$$

The throughput is assumed to be proportional to the cross-sectional area and is defined as Q/t_m, where Q is the amount injected and t_m is the elution time for unretained solute. For comparisons involving isochronic columns, for which this equation was developed, this definition is suitable. However, it is not suitable for comparing RPSF and sphere columns, since these are not, in general, isochronic. In this case, the throughput should be based on the elution time (infinite dilution) of the desired product; i.e., with j as the desired product, $T=Q/t_j^o$. With this definition, Eq. 1 modifies to:

$$T_j = \left[\frac{L}{N^*} - H(u)\right] \frac{4(1+k_j^o)}{\beta_j\, t_j^o} \quad . \tag{2}$$

The throughput in Eq. 2 is based on the time necessary for the tail of the component j zone to exit the column. Strictly speaking, the basis should be the time for a complete cycle. However, the re-equilibration time is dependent on other considerations, and for the purposes of comparison it will be assumed that these are equal for both columns. This assumption will, in general, favor the sphere column, since the higher capacity of this column leads to higher retention times.

Equation 2 can be simplified using the relationship between retention time and capacity factor:

$$t_j^o = \frac{L\varepsilon}{u}(1 + k_j^o) \quad . \tag{3}$$

Substituting Eq. 3 in Eq. 2,

$$T_j = \left[\frac{L}{N^*} - H(u)\right] \frac{4u}{\beta_j L\varepsilon} \quad . \tag{4}$$

The equilibrium parameters k_j^o and β_j in Eqs. 3 and 4 are related to the column capacity, $\bar{q}_j$, through the Langmuir equation:

$$\bar{q}_j = \frac{k_j^o \bar{C}_j}{1 + \beta_j \bar{C}_j} \quad . \tag{5}$$

It is clear from this equation that k_j^o and β_j are dependent on the packing density and will, in general, be different for RPSF and sphere columns. If, however, the capacity is defined on the basis of unit mass (or unit volume) of support, and the fluid concentration on the basis of unit volume of fluid,

$$q_j = \frac{a_j C_j}{1 + b_j C_j} \quad , \tag{6}$$

the equilibrium parameters a_j and b_j are dependent only on the intrinsic thermodynamic adsorption characteristics of the support

and are independent of geometry and packing configuration. Using Eqs. 5 and 6, Eq. 4 can be rewritten as:

$$T_j = \left[\frac{L}{N^*} - H(u)\right] \frac{4\,u}{L\,b_j} \quad . \tag{7}$$

With appropriate equations for the minimum number of stages for a separation, N*, and the plate height, H(u), Eq. 7 can be used for the comparison of throughput in RPSF and sphere columns. For the separation of a component j from i, N* for a RPSF column is given by:

$$N_f^* = 16\left[\frac{(1+ k_j^{o,f})}{k_j^{o,f} - k_i^{o,f}}\right]^2 \quad , \tag{8}$$

and, for a sphere column,

$$N_s^* = 16\left[\frac{(1+ \psi k_j^{o,f})}{\psi(k_j^{o,f} - k_i^{o,f})}\right]^2 \quad , \tag{9}$$

where:

$$\frac{k_j^s}{k_j^f} = \psi = \frac{(1-\varepsilon_s)\varepsilon_f}{(1-\varepsilon_f)\varepsilon_s} \quad . \tag{10}$$

It is clear from Eqs. 8 and 9, that N* is a quantitative measure of the degree of difficulty of a separation, with a larger number signifying a more difficult separation.

An equation widely used for the calculation of plate height in liquid chromatography is (15):

$$H(\bar{u}) = \frac{B}{\bar{u}} + A\bar{u}^{1/3} + C\bar{u} \quad . \tag{11}$$

This equation accounts for the influence of axial diffusion, flow dispersion, and intraparticle mass transfer on separation.

Equations 7-11 are the equations required for predicting the performance characteristics of sphere and RPSF columns as a function of operating conditions. However, certain experimental data must first be available. Specifically, the thermodynamic adsorption parameters for a model biomolecule (k_j^o and b_j) and the column packing characteristics (ε_s and ε_f) must be known. Also, the coefficient A in Eq. 11 must be experimentally measured for the RPSF column; all other coefficients in this equation, for both the sphere and RPSF column, are available or can be estimated.

EXPERIMENTAL MATERIALS AND METHODS

Materials

Silica PAE 1000, a commercial chromatographic anion-exchange support, was purchased from Amicon (Danvers, MA, USA). This is a macroporous, spherical support with a nominal diameter of 10 μm. Q-106 quartz fiber (Manville Sales, Toledo, OH, USA) was used as the substrate for the synthesis of the ion-exchange fiber packing. This fiber is 98.5% (w/w) silica and has a nominal diameter of 0.7 μm.

Reagents

3-Glycidoxypropyltrimethoxysilane (Z-6040) was purchased from Aldrich (Milwaukee, WI, USA). Polyethyleneimine (PEI 6) was supplied by Polysciences (Warrington, PA, USA). All solvents (acetone, methanol, etc.) and reagents (sulfuric acid, nitric acid, etc.) were purchased from Fischer Scientific (Cincinnati, OH, USA). The protein bovine serum albumin (BSA) was obtained from Sigma (St. Louis, MO, USA).

Apparatus

A SP8800 ternary gradient HPLC system (Spectra Physics, San Jose, CA, USA) was used for the determination of dispersion effects in the RPSF column. Absorbance was monitored with a Spectra-Physics Spectra 100 variable wavelength detector. Adsorption capacity measurements were made with a Shimadzu UV-160U spectrophotometer (Shimadzu Scientific Instruments, MD, USA).

Synthesis of RPSF Column

The ion-exchange RPSF column was synthesized using the method developed by King and Pinto (10). Briefly, the Q-106 fiber was first cut in water with a homogenizer (Biospec Products, Bartlesville, OK, USA) to a length of 115 μm. The fiber was then cleaned by washing with acetone and deionized water and hydroxylated in a 50:50 (v/v) mixture of concentrated sulfuric acid for 8 h. The fiber was rewashed thoroughly with deionized water, and dried in a vacuum oven at 110 °C for 2 h. The dried fiber was then functionalized by reacting with a PEI 6 solution, and cured by vacuum drying.

Column Packing

The anion-exchange fiber was packed into a standard HPLC column (150 mm x 4.6 mm I.D.) using a two-step procedure of sedimentation followed by pressurization. The column was vertically oriented, and fiber suspended in methanol was poured into the top end. A weak vacuum was applied at the bottom to remove solvent. Pressurization of the column was at 2400 psi, applied for 5 min. The sedimentation/pressurization process was repeated until the column was full and tightly packed.

Measurement of Protein Capacity

The BSA adsorption capacity of the PAE 1000 support was determined with a batch method. Solution conditions for these

measurements were pH 8 and 0.12 M NaCl. The first step of the method was equilibration of a weighed quantity of adsorbent with a 0.12 M salt solution for 2 h. Subsequently, the support was washed repeatedly with deionized water and centrifuged. A protein solution of known concentration was then added to the support, and the mixture was agitated for 2 h; preliminary experiments had established that this was sufficient time for equilibration. After equilibration the ion exchanger was spun down, and the supernatant was sampled and analyzed using the spectrophotometer at 280 nm. From the change in concentration of the solution, the amount adsorbed was determined.

Isocratic Elution Characteristics

The flow dispersion characteristics of the RPSF column were determined from the isocratic elution of BSA at pH 8 and 0.12 M NaCl. Tris-HCl was used as the buffer. The injected protein solution concentration was 5 mg/mL, and a sample volume of 15 μL was used in all cases. Three volumetric flow rates of 1, 2, and 3 mL/min were used. The column response was monitored at 280 nm.

EVALUATION OF PLATE HEIGHT COEFFICIENTS

The first term on the right-hand side of Eq. 11 accounts for axial molecular diffusion, and the coefficient of this term is given by (16):

$$B = 2\lambda(1 + k^{o}) D_m , \tag{12}$$

where λ is a constant. Based on experimental observations, for a sphere column, Eq. 12 is commonly approximated as:

$$B^{s} = 2 D_m . \tag{13}$$

For a fiber column, from Eqs. 10 and 11,

$$B^f = 2\lambda\left(1 + \frac{k^{o,s}}{\psi}\right) D_m \quad . \tag{14}$$

Since in practice $\psi > 1$ and $k^{o,s}$ is positive, $2\lambda\left(1 + \frac{k^{o,s}}{\psi}\right)$ will be less $2\lambda(1 + k^{o,s})$. Thus, assigning $2\lambda\left(1 + \frac{k^{o,s}}{\psi}\right) = 2$ will give a larger than actual estimate for the contribution of axial diffusion to the plate height, and, hence, a conservative estimate for the performance of the fiber column (Eq. 7). Using this approximation,

$$B^f = 2\, D_m \quad . \tag{15}$$

The second term on the right-hand side of Eq. 11 accounts for the contribution of flow anisotropy to the plate height, and the coefficient A is calculated from:

$$A = \bar{A}\, d\left[\frac{d}{D_m}\right]^{1/3} \quad . \tag{16}$$

For a sphere column, the value typically used for $\bar{A}$ is 1 (13). The $\bar{A}$ for the fiber column was estimated from the isocratic elution data for BSA on the ion-exchange RPSF column. A typical column response is shown in Figure 1. Since the fiber support is nonporous and the concentration is in the linear region of the isotherm, the band broadening is due to flow dispersion and axial diffusion only. Thus, from Eq. 11,

$$H(\bar{u}) = \frac{B}{\bar{u}} + A\bar{u}^{1/3} \quad , \tag{17}$$

and a plot of $\bar{u}\, H(u)$ vs $\bar{u}^{\frac{4}{3}}$ should be a straight line with slope A. The plate height was calculated from the first and second moments of the peaks using the equation:

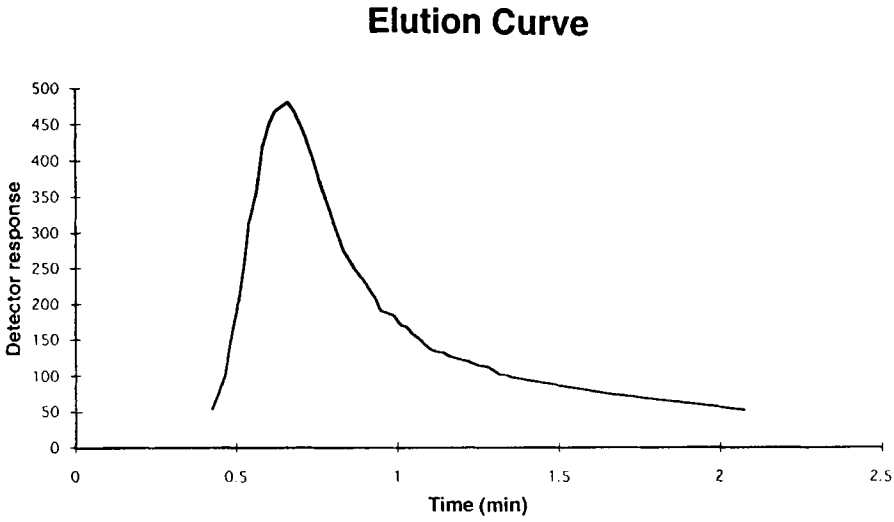

FIGURE 1. Typical Elution Chromatogram for BSA on RPSF Column.

$$H(u) = \frac{\sigma^2 L}{\mu^2} \quad . \tag{18}$$

Figure 2 is a plot of the experimental plate height for the RPSF column as a function of velocity. A strong linear relationship is obtained with a linear regression coefficient of 0.9975. The slope of this line was used in Eq. 16 to calculate an $\bar{A}$ value of 24.4 for the RPSF column; the diffusion coefficient of BSA was obtained from the literature as 7×10^{-7} cm^2/s (17). The much larger $\bar{A}$ for the RPSF column, as compared to the sphere column, indicates a lower packing uniformity, which is as expected. Substituting the values of $\bar{A}$ for the sphere and RPSF columns in Eq. 16,

$$A^s = d_s \left[\frac{d_s}{D_m}\right]^{1/3} \quad , \text{ and} \tag{19}$$

$$A^f = 24.4\ d_{f,e} \left[\frac{d_{f,e}}{D_m}\right]^{1/3} \quad . \tag{20}$$

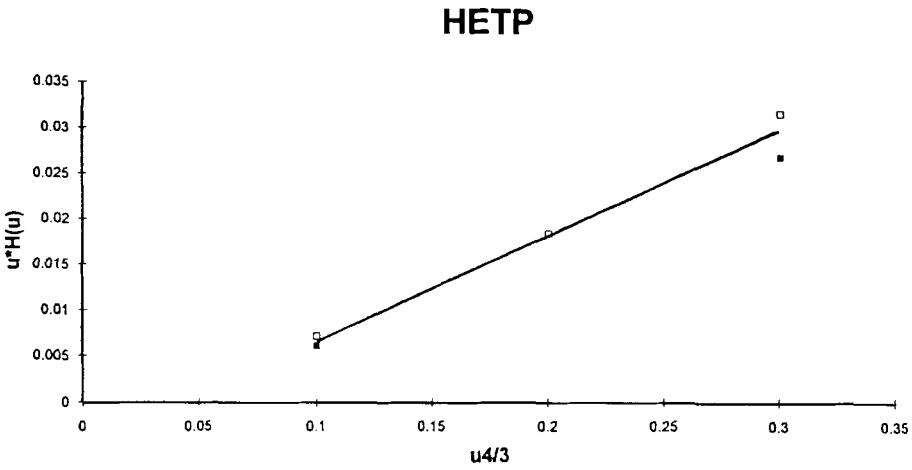

FIGURE 2. Plate Height - Velocity Plot for the Calculation of Flow Dispersion in RPSF Column.

The contribution of the mass-transfer resistance to plate height is accounted for by the third term on the right-hand side of Eq. 11. For a sphere column, the coefficient C can be calculated from (16):

$$C^s = \left(q'_s \left[\frac{k''_s}{(1 + k''_s)^2} \right] \frac{D_m}{D_p} \right) \frac{d_s^2}{D_m} = \bar{C}^s \frac{d_s^2}{D_m} . \qquad (21)$$

Equivalently, for a fiber column (16),

$$C^f = \left(q'_f \left[\frac{k''_f}{(1 + k''_f)^2} \right] \frac{D_m}{D_p} \right) \frac{d_f^2}{D_m} = \bar{C}^f \frac{d_f^2}{D_m} . \qquad (22)$$

The relative values of $\bar{C}^s$ and $\bar{C}^f$ can be estimated from a comparison of terms in Eqs. 21 and 22. When comparing the performance of the two columns, it will be assumed that the adsorbents are identical, except for the difference in their

macroscopic geometry. Also, the systems will be compared for identical mobile-phase conditions. Thus, the solute diffusivities in the liquid and solid phases, D_m and D_p, will be the same for both supports. With regard to the equilibrium term in the box bracket, since the ratio of the stationary zone to the mobile zone is less in a RPSF column than in a sphere column, $k''_f < k''_s$. This implies:

$$\left[\frac{k''_s}{(1 + k''_s)^2}\right] > \left[\frac{k''_f}{(1 + k''_f)^2}\right] . \tag{23}$$

Thus, the contribution of this term to plate height is larger for the sphere column than for the RPSF column. However, once again, in order to ensure a conservative estimate for the performance of the latter, it will be assumed that these terms are equal. With this consideration, substituting the values for $q'_f = 1/16$ and $q'_s = 1/30$ (16), Eqs. 21 and 22 give:

$$\bar{C}_f = \frac{15}{8} \bar{C}_s . \tag{24}$$

The value of $\bar{C}_s$ commonly used is 0.1 (13). Therefore, from Eq. 24, $\bar{C}_f = 0.1875$. Substituting in Eqs. 21 and 22,

$$C^s = 0.1 \frac{d_s^2}{D_m} , \tag{25}$$

and

$$C^f = 0.1875 \frac{d_f^2}{D_m} . \tag{26}$$

The plate height can now be expressed in terms of system and operating parameters. Rewriting Eq. 11 in terms of the superficial velocity and substituting Eqs. 13, 19, and 25, the plate height in a sphere column is:

$$H^s = \frac{2D_m\varepsilon_s}{u} + d_s\left[\frac{d_s u}{D_m \varepsilon_s}\right]^{1/3} + 0.1\,\frac{d_s^2 u}{D_m \varepsilon_s}. \qquad (27)$$

Similarly, for an RPSF column substituting Eqs. 14, 20, and 26,

$$H^f = \frac{2D_m\varepsilon_f}{u} + 24.4d_{f,e}\left[\frac{d_{f,e} u}{D_m \varepsilon_f}\right]^{1/3} + 0.1875\,\frac{d_f^2 u}{D_m \varepsilon_f}. \qquad (28)$$

RESULTS AND DISCUSSION

In order to establish the importance of support geometry on column throughput, it is necessary to compare RPSF and sphere columns packed with supports that are physically and chemically identical, with the only difference being their macroscopic geometry. Thus, for example, the two supports will have the same thermodynamic adsorption characteristics and the same porous structure. While it is recognized that the synthesis of such identical supports is in practice difficult, they provide a useful theoretical paradigm for examining the influence of macroscopic geometry on performance.

The model parameters chosen for the comparison are shown in Table 1. The fiber dimensions selected match the dimensions of the prototype silica fiber of this study. The 10-μm sphere has been selected as an initial basis for comparison, and the effects of particle diameter will be considered later. The bed porosities in Table 1 were obtained experimentally for the RPSF and the PAE 1000 columns. The equilibrium coefficients are from the batch isotherm measurements of BSA on PAE 1000. These characteristics have been assigned to both supports, since, as was stated earlier, identical thermodynamic adsorption characteristics are being assumed. The diffusivity of BSA in the liquid was obtained from the literature (17), at conditions close to those used for the equilibrium measurements (0.12 M NaCl, pH 8).

TABLE 1. MODEL PARAMETERS USED FOR COMPARISON OF THROUGHPUT

Parameter	Sphere Packed Column	RPSF Column
Packing Diameter (μm)	10	0.7
Packing Length (μm)	-	115
Bed Porosity	0.29	0.79
Capacity Factor k^{o}_{i}	4.95	4.95
Langmuir Coefficient b_i (ml/mg)	0.13	0.13
BSA Liquid Diffusivity (cm^2/s) x 10^7	7.0	7.0

It is clear from Eqs. 8 and 9 that the minimum number of plates N* is dependent on the capacity factor of the product and the difference between the capacity factor of the product and contaminant. For the BSA\PAE-1000 system, the dependence of N^*_s on the degree of difficulty of the separation is given in Table 2. The ratio of the capacity factors (k^o_j/k^o_i) is a direct measure of the difficulty of separation. Thus, a ratio of 10 indicates that the support has a very strong affinity for BSA relative to the contaminant, while 1.2 signifies comparable affinities.

In general, for a given separation, the minimum number of stages necessary in an RPSF column will be different from that in a sphere column, due to the difference in the bed porosities. This difference in the N* values is dependent on the magnitude of the capacity factor of the product (k^o_j). It can be shown from Eqs. 8 and 9, that for the system of Table 1, if $k^{o,f}_j >> 1$,

$$N^*_s \cong N^*_f \quad . \tag{29}$$

Also, when $k^{o,f}_j = 1$,

TABLE 2. MINIMUM NUMBER OF STAGES NECESSARY FOR BSA SEPARATION

k_j^o/k_i^o	10	2	1.5	1.2
N_s^*	28	92	208	832

$$N_s^* = 0.31\ N_f^* \ . \tag{30}$$

The comparison of the throughput of the two columns was made by substituting the appropriate equation for plate height (Eq. 27 or 28) in Eq. 7. The calculations were performed for three column lengths, 5, 15, and 25 cm. The throughput was determined as a function of velocity and N*. With regard to N*, the value of N_s^* was fixed to specify the difficulty of separation, and the corresponding value of N_f^* was calculated from either Eq. 29 or 30, depending on the case being considered, $k_j^{o,f} >> 1$ or $k_j^{o,f} = 1$; these two cases cover the useful range of retention behavior from strongly retained to weakly retained.

Shown in Table 3 is the throughput predicted for a product j when separated from a contaminant i on a 25-cm column with $k_j^{o,f} >> 1$. As calculated, the throughputs are for 100% recovery of product at 100% purity. The upper limit for the velocity was determined from the Leva equation (18), based on a maximum column pressure drop of 6000 psi. For a 25-cm RPSF column, the maximumvelocity is 0.8 cm/s, while for a sphere column of equal length, it is 0.5 cm/s. The range used for N*, 50 to 1000 plates, was based on the data in Table 2 to ensure physically realistic values.

The results in Table 3 show that for both columns, at every N*, there is an optimum velocity for maximum throughput. Also, this velocity is not, in general, the maximum velocity attainable.

TABLE 3. COMPARISON OF THROUGHOUT IN RPSF AND SPHERE COLUMNS FOR $k_j^{o,f} >> 1$ AND A 25 cm COLUMN

u (cm/s)	$T \times 10^3$ (mg cm^{-2} s^{-1})							
	N*							
	50		150		250		1000	
	Sphere	Fiber	Sphere	Fiber	Sphere	Fiber	Sphere	Fiber
0.001	0.801	0.786	0.264	0.250	0.157	0.143	0.036	0.022
0.005	3.981	3.880	1.298	1.201	0.761	0.666	0.157	0.063
0.01	7.910	7.692	2.544	2.334	1.471	1.262	0.263	0.056
0.025	19.43	18.92	6.011	5.529	3.328	2.850	0.309	0.0
0.05	37.76	37.24	10.93	10.45	5.560	5.094	0.0	0.0
0.10	71.28	72.95	17.62	19.37	6.890	8.653	0.0	0.0
0.25	147.3	175.7	13.16	41.73	0.0	14.94	0.0	0.0
0.50	193.2	338.0	0.0	70.10	0.0	16.52	0.0	0.0
0.80	0.0	523.0	0.0	94.38	0.0	8.652	0.0	0.0

$N^* = N_s^* = N_f^*$

This is clearly illustrated in Figures 3 and 4. It should be noted that in some cases, for example RPSF with N* = 50, the maximum is not obtained because it occurs at a velocity higher than is physically attainable due to pressure drop limitations.

If the maximum throughput in the two columns is compared for the difficult separation case, represented by N* = 1000, the sphere column is greatly superior, giving a maximum throughput of 5 times that of the RPSF column. This is due to the requirement, inherently imposed by a difficult separation, of a very short plate height. Referring to Eqs. 27 and 28, for velocities of practical interest, the contribution of axial molecular diffusion to plate height is negligible, and only the contributions of flow dispersion and mass transfer are significant. For separations requiring a very short plate height, the significant terms impose the constraint of a low velocity. At low velocities, the dispersion term dominates, and since at equal velocities the dispersion contribution to plate height for a spherical support is

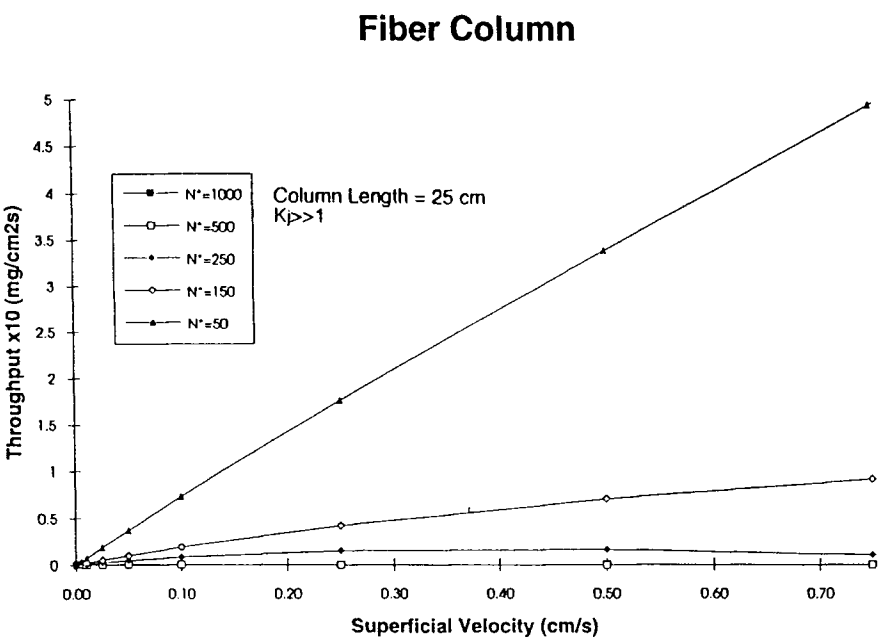

FIGURE 3. Effect of Velocity on Throughput in an RPSF Column.

much smaller than for a fibrous support, the former gives a superior throughput.

For easier separations, the situation is reversed. In this case, complete separation can be achieved with a larger plate height, and, thus, higher velocities can be used. At higher velocities, the mass-transfer contribution to plate height dominates, and the mass-transfer contribution is much smaller for the fiber column. This advantage is sufficient to overcome the poorer dispersion characteristics, resulting in a higher throughput. For example, in Table 3 for N* = 150, the maximum throughput of the RPSF column is 5 times that of the sphere column.

The capacity factor of the product, k_j^o, also has a strong influence on the relative performance of the columns. Table 4

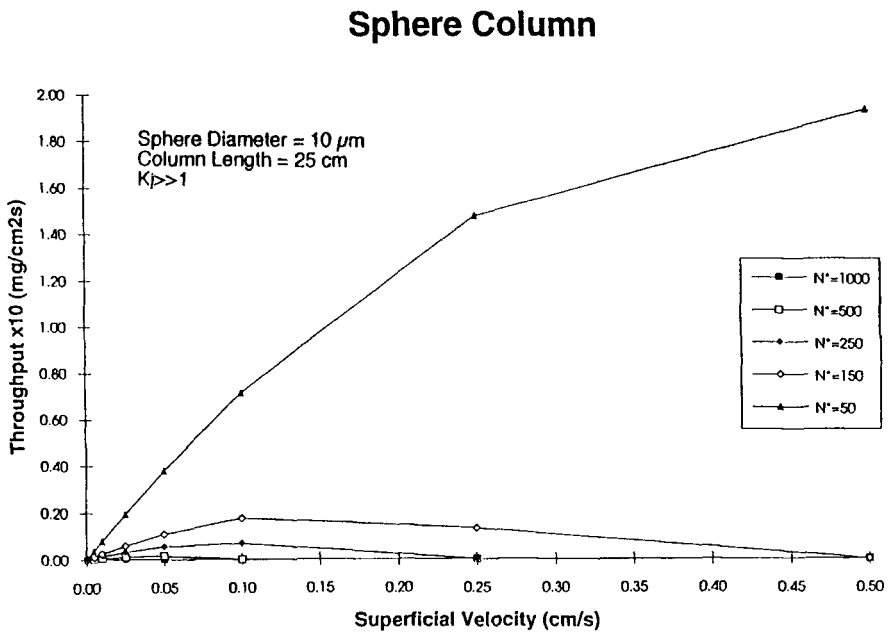

FIGURE 4. Effect of Velocity on Throughput in a Sphere Column.

TABLE 4. COMPARISON OF THROUGHPUT IN RPSF AND SPHERE COLUMNS FOR $k_j^{o,f} = 1$ AND A 25 cm COLUMN

u (cm/s)	T x 10^3 (mg cm^{-2} s^{-1})							
	N*							
	50		150		250		1000	
	Sphere	Fiber	Sphere	Fiber	Sphere	Fiber	Sphere	Fiber
0.001	2.878	1.572	0.956	0.500	0.572	0.286	0.139	0.045
0.005	14.36	7.761	4.756	2.403	2.834	1.331	0.672	0.126
0.01	28.67	15.38	9.454	4.667	5.611	2.524	1.287	0.113
0.025	71.29	37.85	23.25	11.06	13.64	5.701	2.830	0.0
0.05	141.4	74.48	45.28	20.90	26.06	10.19	4.443	0.0
0.10	278.0	145.9	85.87	38.74	47.43	17.31	4.419	0.0
0.25	660.8	351.4	180.3	83.46	84.28	29.88	0.0	0.0
0.50	1209	676.0	248.1	140.2	55.93	33.04	0.0	0.0
0.80	0.0	1046	0.0	188.8	0.0	17.3	0.0	0.0

$N^* = N_s^* = 0.31\ N_f^*$

summarizes the results for the case $k_j^{o,f} = 1$. The general trends observed for $k_j^{o,f} >> 1$ are once again evident. However, there are two significant differences. First, the maximum throughputs that can be obtained for each N* are higher at the lower capacity factor. This is to be expected with components that are less strongly retained, since it reduces the total time for separation. Secondly, the advantage of the RPSF column for lower N* separations is lost. This is seen more clearly from Figure 5. Plotted in this figure is the ratio of the maximum throughput of the fiber column to the sphere column as a function of N* for $k_j^{o,f} >> 1$ and $k_j^{o,f} = 1$. It can be seen that at the higher value of the capacity factor, the fiber column gives a higher throughput up to an N* value of approximately 350. However, for $k_j^{o,f} = 1$, though the RPSF column gives comparable throughputs at N* of 50 and 150, it offers no advantage over the conventional system. This difference can be explained from the effect of the capacity factor on N*. When the capacity factor is large, the minimum number of plates necessary for a given separation is essentially the same for both columns (Eq. 29). On the other hand, when the capacity factor is small, the sphere column is more efficient, requiring a smaller number of plates to achieve the same separation (Eq. 30). Consequently, for the latter case, when columns of equal length are being compared, the fiber column must have a significantly shorter plate height in order to be competitive with the sphere column. This can only be achieved with the combination of a low N* value and high linear velocities. However, even for relatively simple separations, the necessary velocities are higher than can be tolerated in the RPSF column due to pressure drop.

The effect of column length on throughput is shown in Figure 6 for the RPSF column; the behavior of the sphere column is characteristically identical. As is evident, the throughput is a strong function of the column length. The maximum throughput attainable is decreased as the column length increases, and the optimum velocity also decreases. If the column length is too short

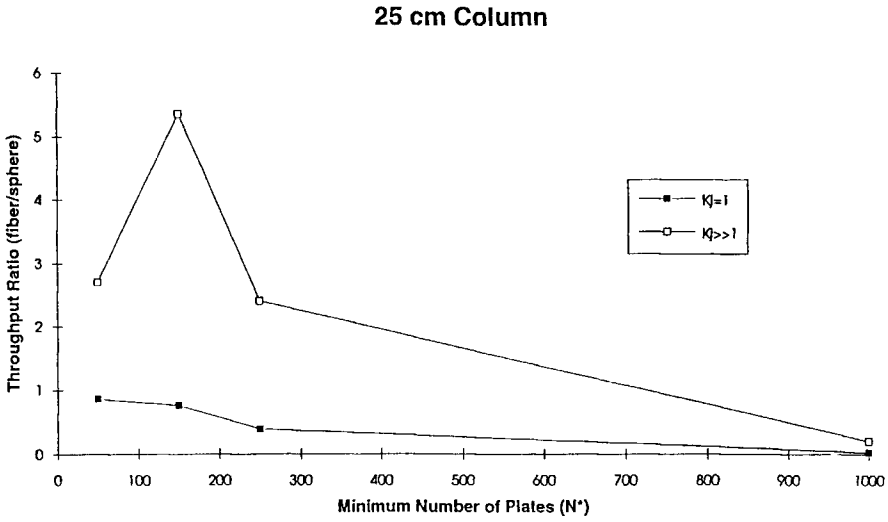

FIGURE 5. Comparison of Throughput in RPSF and Sphere Columns as a Function of Difficulty of Separation.

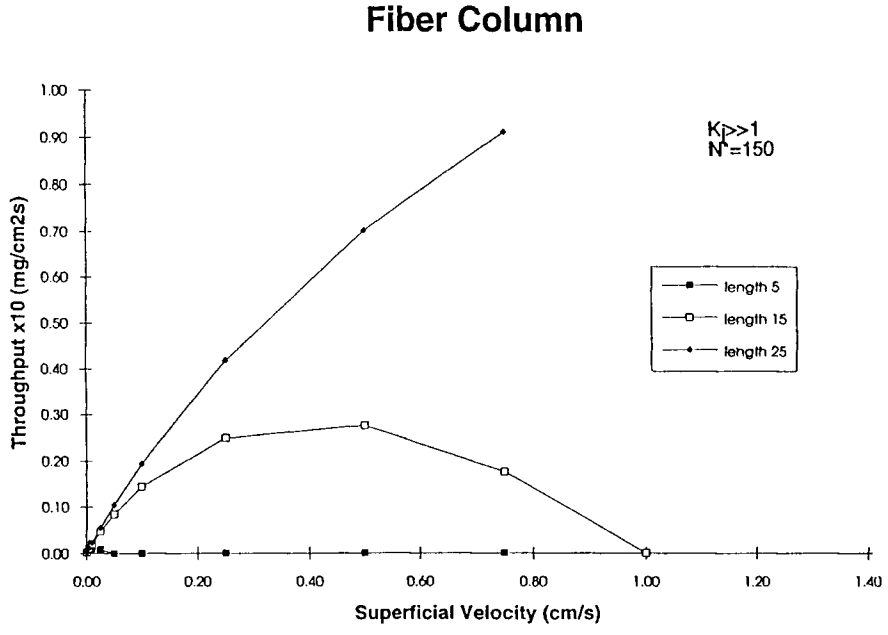

FIGURE 6. Effect of Column Length on Throughput in an RPSF Column.

to meet the minimum number of plates requirement, as is the case for the 5-cm column, no product is produced.

From the results in Tables 3 and 4, it is clear that the combination of a lower pressure drop and more efficient intraparticle mass transfer in RPSF columns offers an advantage for certain separations. However, it is not clear whether this advantage stems from the higher velocity limit or better mass transfer. If a higher velocity limit is largely responsible, then RPSF columns may offer no real advantage, even for low N*-high k_j^o separations, since higher velocities can be attained in sphere columns by simply increasing the diameter of the particle. Thus, it is important to compare the performance of the RPSF column with larger-diameter sphere columns. Two sphere diameters of 50 μm and 100 μm were selected for this purpose. For these diameters and a column porosity of 0.29, the upper limits for velocity in a 25-cm column are 10 cm/s and 40 cm/s, respectively. These are considerably higher than for the RPSF column.

Figure 7 shows the throughputs for 25-cm columns packed with the larger-diameter spherical supports. The predictions are for N* = 50 and $k_j^{o,f} >> 1$, because these are typical conditions at which the RPSF column has been shown to perform better than the 10-μm sphere column. Plotted as a reference in Figure 6 is the throughput obtained with the 10-μm sphere column. Clearly, the performance of the larger-diameter supports is inferior to that of the 10-μm sphere, and, thus, to the RPSF column. Notice that the optimum velocity is very small, making the higher velocity limit an irrelevant advantage; the mass-transfer characteristics for larger supports are poor, and the system cannot be operated at higher velocities, as is the case for the RPSF column.

SUMMARY

A theoretical comparison has been made of the performance of RPSF columns with conventional chromatographic columns. It has

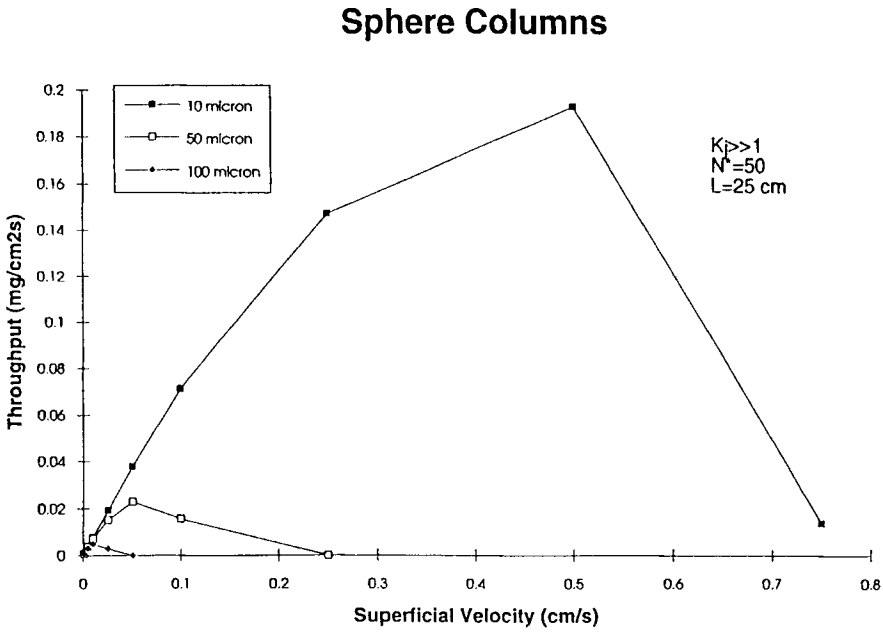

FIGURE 7. Effect of Diameter of Spherical Packing on Column Throughput.

been shown that for separations performed on an adsorbent that has a strong affinity for product over contaminants, chromatographic elution separations on a RPSF column will give considerably higher throughputs. This is due primarily to more efficient intraparticle mass transfer.

With respect to the practical significance of RPSF columns, they appear to be ideal for affinity separations. These separations are characterized by a high capacity factor for the product and large capacity factor ratios of product to contaminants. Unfortunately, there are currently no suitable RPSF supports available for this application. The key requirements for a suitable support are a submicron radial dimension, macroporosity, and sufficient accessible adsorption area to provide capacities comparable to conventional adsorbents for

biomolecules. The synthesis of such a support is the next technical challenge in the development of RPSF columns.

LIST OF SYMBOLS

a	Langmuir coefficient (volume fluid/weight adsorbent)
A	coefficient for flow dispersion
$\bar{A}$	constant (Eq. 16)
b	Langmuir coefficient (volume fluid/mass)
B	coefficient for axial diffusion
C	mass dispersion coefficient
$\bar{C}$	coefficient defined by Eqs. 21 or 22
C_j	concentration of species j in fluid (mass/volume fluid)
$\bar{C}_j$	concentration of species j in fluid (mass/volume column)
d	diameter of particle
$d_{f,e}$	diameter of sphere with same volume as fiber
D_m	diffusivity in fluid
D_p	diffusivity in particle
$H(u)$	plate height
k^o	capacity factor (infinite dilution)
$k^{o,f}$	capacity factor in fiber column (infinite dilution)
$k^{o,s}$	capacity factor in sphere column (infinite dilution)
k''	equilibrium distribution ratio
L	column length
N^*	minimum number of plates
q	concentration in stationary phase (mass/weight adsorbent)
$\bar{q}$	concentration in stationary phase (mass/volume column)
q'	constant, dependent on particle geometry
t^o	retention time (infinite dilution)
t_m	retention time for unretained solute
T	throughput
u	superficial velocity
$\bar{u}$	interstitial velocity

Greek Symbols

β	equilibrium parameter, defined by Eq. 5
ε	bed porosity
λ	constant (Eq. 12)
μ	first moment
σ^2	second central moment
ψ	capacity factor ratio (Eq. 10)

Superscripts

f	fiber
s	sphere

Subscripts

f	fiber
i	species i
j	species j
s	sphere

ACKNOWLEDGMENTS

This work was supported by the National Science Foundation under Grant No. CTS-9207631. This support is gratefully acknowledged.

REFERENCES

1. National Research Council, Report from Committee on Chemical Engineering Frontiers, Frontiers in Chemical Engineering, National Academy Press, Washington D.C. (1988).

2. M. R. Ladisch, in Advanced Biochemical Engineering, H.R. Bungay and G. Belfort, Eds., John Wiley, New York, 1987, p. 219.

3. R.K. Scopes, Protein Purification, 2nd ed., Springer-Verlag, New York, (1987).

4. H.A. Chase, in Plant and Animal Cells: Process Possibilities, C. Webb and F. Mavituna, Eds., Ellis Horwood, Chichester, U.K., 1987.

5. V. Saxena and M. Dunn, Bio/Technology 8, 250 (1989).

6. H. Ding, M.C. Yang, D. Schisla, and E.L. Cussler, AIChE J. 35, 814 (1989).

7. N.B. Afeyan et al., Bio/Technology 8, 203 (1990).

8. T.B. Tennikova, B.G. Belenki, and F. Svec, J. Liq. Chromatogr. 13, 63 (1990).

9. P. Wikstrom and P. Larrson, J. Chromatogr. 388, 123 (1987).

10. J.K. King and N.G. Pinto, J. Chromatogr. 609, 61 (1992).

11. A. Singh and N.G. Pinto, Reactive Polymers, accepted for publication (1994).

12. K.K. Unger, W. Messer, and K.F. Krebs, J. Chromatogr. 149, 1 (1978).

13. J.H. Knox and H.M. Pyper, J. Chromatogr. 363, 1 (1986).

14. L.R. Snyder, J.W. Dolan and G.B. Cox, J. Chromatogr. 483, 63 (1989).

15. J.H. Knox, J. Chromatogr. Sci. 15, 352 (1977).

16. J.C. Giddings, Dynamics of Chromatography: Part I, Marcel Dekker, New York (1965).

17. E.E. Graham and C.F. Fook, AIChE J. 28, 245 (1982).

18. M. Leva, Chem. Eng. 56, 115 (1949).